Geophysical Research Letters

Evidence for an Oceanic Source of Methyl Ethyl Ketone to the Atmosphere

J. F. Brewer[1] , E. V. Fischer[1] , R. Commane[3] , S. C. Wofsy[4,5] , B.C. Daube[4], E. C. Apel[6] , A. J. Hills[6], R. S. Hornbrook[6] , B. Barletta[7], S. Meinardi[7], D. R. Blake[7] , E. A. Ray[8,9] , and A. R. Ravishankara[1,2]

[1]Department of Atmospheric Science, Colorado State University, Fort Collins, CO, USA, [2]Department of Chemistry, Colorado State University, Fort Collins, CO, USA, [3]Department of Earth and Environmental Sciences, Lamont-Doherty Earth Observatory and Columbia University, Palisades, NY, USA, [4]Harvard John A. Paulson School of Engineering and Applied Sciences, Harvard University, Cambridge, MA, USA, [5]Department of Earth and Planetary Sciences, Harvard University, Cambridge, MA, USA, [6]Atmospheric Chemistry Observations and Modeling Laboratory, National Center for Atmospheric Research, Boulder, CO, USA, [7]Department of Chemistry, University of California, Irvine, Irvine, CA, USA, [8]Chemical Sciences Division, NOAA Earth System Research Laboratory, Boulder, CO, USA, [9]Cooperative Institute for Research in Environmental Sciences, University of Colorado, Boulder, CO, USA

Abstract Methyl ethyl ketone (MEK) is a relatively abundant but understudied oxygenated volatile organic compound that can serve as a source of both HO_x and PAN when photooxidized. We use aircraft observations of MEK from the remote marine troposphere to show that the ocean serves as a source of MEK to the atmosphere during both meteorological winter and summer. There is pronounced seasonality in the MEK profiles in the extratropical troposphere, with higher MEK mixing ratios observed in summer than in winter. MEK in clean air over the remote oceans correlates with both acetone and acetaldehyde, whose primary sources in the ocean water are the photooxidation of organic material. We show that even a small (>1 nM) concentration of MEK in surface waters is sufficient to allow the ocean to be a net source of MEK to the atmosphere over ocean basins across multiple seasons.

Plain language summary Methyl ethyl ketone (MEK) is an abundant but understudied gas in Earth' atmosphere, which is emitted into the atmosphere from both human and natural sources. When MEK is broken apart by ultraviolet sunlight, the products released by those reactions play important roles in the formation and destruction of air pollution. In this paper, we show that the oceans are a source of MEK to the atmosphere. The oceanic emissions we document correlate strongly with some other gases that are known to be produced in the ocean but not those most closely associated with the growth of microscopic oceanic phytoplankton. Finding this new source helps us better understand the importance of MEK to the atmosphere and provides guidance for future oceanic and atmospheric research.

1. Introduction

Ketones are important to atmospheric oxidation because they are ubiquitous oxygenated volatile organic compounds (OVOCs) that have a sufficiently long atmospheric lifetime to be transported to the upper troposphere. There, photolysis of acetone (and other carbonyls such as CH_2O) can serve as an additional source of hydroxyl radicals ($HO_x = OH + HO_2$) in a region where water vapor is scarce (McKeen et al., 1997; Neumaier et al., 2014; Singh et al., 1995; Wennberg et al., 1998). The significance of methyl ethyl ketone (MEK, 2-butanone), the second most abundant atmospheric ketone, remains uncertain (Singh et al., 2004; Yañez-Serrano et al., 2016). Similar to acetone, MEK photolysis in the near-ultraviolet can produce HO_x radicals and PAN precursors (Brewer et al., 2019; Martinez et al., 1992; Romero et al., 2005). The number of HO_x produced by photolysis of each MEK in the upper troposphere should be comparable to or higher than that from each acetone molecule in this region. The exact yield of HO_x will depend on the concentration of NO and the quantum yields in the photolysis of MEK at UT pressures and temperatures. The sources of MEK are not fully understood (Yañez-Serrano et al., 2016). Known sources of MEK include direct emissions from biomass burning and the terrestrial biosphere, as well as secondary production from the oxidation of anthropogenic alkanes (Cappellin et al., 2016; Jordan et al., 2009; Yañez-Serrano et al., 2016). Better quantification of the sources of MEK is needed to constrain the abundances, seasonality, and transport of MEK throughout the atmosphere (Chen et al., 2019).

Many volatile organic compounds (VOCs) are emitted from the ocean surface from a variety of biogenic and abiogenic sources. Dimethyl sulfide (DMS), a crucial contributor to the global sulfur cycle and particle formation, is produced by phytoplankton in seawater (Challenger, 1952; Lovelock et al., 1972). The production of DMS is so tightly coupled to oceanic productivity that seabirds use it as a cue to find prey in the open ocean (Nevitt et al., 1995). Other VOCs have primarily photochemical sources in the ocean: Acetaldehyde in the surface ocean has been shown to originate from the photolysis of chromophoric dissolved organic matter (CDOM; Kieber et al., 1990; Millet et al., 2010; Wang et al., 2019). VOCs such as methyl nitrate (CH_3ONO_2) have potentially more complicated oceanic sources. While the primary oceanic production of methyl nitrate is likely to be the photolysis of CDOM (Fisher et al., 2018; Moore & Blough, 2002), the distribution of methyl nitrate in the water column suggests the possibility of additional biological sources (Moore & Blough, 2002). Acetone has been shown to have a large oceanic emission (Fischer et al., 2012; Yang et al., 2014, 2016). Acetone is known to be produced by CDOM photolysis in seawater (Dixon et al., 2013, 2014; Kieber et al., 1990; Zhou & Mopper, 1997), while biological production has been demonstrated in laboratory studies and is considered likely to occur in the ocean as well (Dixon et al., 2013, 2014; Nemecek-Marshall et al., 1995). The two processes are not exclusively independent: In mesocosm experiments on phytoplankton blooms, Sinha et al. (2007) found that the largest fluxes of acetone occurred during the bloom decline phase, marked by relatively high phytoplankton abundance, with less acetone during the low-biomass post-bloom phase. Based on these findings, it is likely that MEK could also have varied oceanic sources.

2. Methods

2.1. Observations of MEK

We use observational data from the first two deployments of the NASA Atmospheric Tomography (ATom) mission. The ATom project is a global survey of atmospheric chemistry, which offers a representative investigation of the composition of the remote atmosphere without the risk of bias incurred in aircraft campaigns designed to investigate specific phenomena (e.g., smoke plumes, continental pollution outflow, and tropospheric process studies). ATom flights consisted of a series of ascending and descending profiles along the flight track to create a tomography of the atmosphere. The ATom-1 and ATom-2 missions took place from 29 July to 23 August 2016, and 26 January to 21 February 2017, respectively.

MEK, acetaldehyde, and acetone concentrations are available for every 2 min during ATom using the Trace Organic Gas Analyzer (TOGA) (Apel et al., 2015; Wang et al., 2019). Sampling for the abundances of methyl nitrate and DMS from the Whole Air Sampler (WAS) (Barletta et al., 2011; Colman et al., 2001) was manually controlled and unevenly spaced in time, but it averaged one measurement every ~3 min. WAS samples were shipped back to the laboratory at UC Irvine and analyzed with gas chromatography (Colman et al., 2001). The lower limits of detection for MEK, acetaldehyde, and acetone are 1, 5, and 5 ppt, while those for DMS and methyl nitrate are 0.1 and 0.01 ppt, respectively. Earlier versions of TOGA had difficulty measuring some carbonyls in clean-air conditions (including acetone and acetaldehyde; Apel, 2003); however, neither the original studies nor more recent updates have suggested that there are any issues in measuring MEK. Changes to TOGA have lowered detection limits and increased the capability of the instrument in measuring carbonyl mixing ratios in clean conditions (Apel et al., 2015; Wang et al., 2019). Further discussion of the tests performed regarding these measurement artifacts in preparation for the ATom campaigns can be found in the supplementary material to this work (for MEK and acetone) and in the supplement to Wang et al. (2019). Data from both WAS and TOGA registering below the lower limit of detection (LLOD) were dynamically assigned a value between 0 and the LLOD as a linear function of how many LLOD-flagged values were recorded on a given flight: the more LLOD-flagged non-NA observations, the closer the assigned value was to 0. This methodology did not change any of the conclusions relative to filling LLOD data with half the LLOD, another common strategy. Because TOGA and WAS measurements were taken at different timesteps, we group the data from both instruments into 1-km vertical bins on ascent and descent of each flight. Carbon monoxide (CO), also used in this analysis, was measured using a Quantum Cascade Laser Spectrometer (Accuracy 3.5 ppb, 0.15 ppb precision at 1 s) (Santoni et al., 2014) and was essentially continuous with a 1-s resolution.

MEK has an estimated atmospheric lifetime against OH oxidation of ~5–6 days at a 24-hr mean OH concentration of ~1.5×10^6 cm^{-3} (Jordan et al., 2009; Yañez-Serrano et al., 2016); its most important alkane

precursors (*n*-butane and *i*-pentane) have mean atmospheric lifetimes against OH oxidation of up to 2–4 days under the same OH concentrations, with longer lifetimes on the order of weeks possible during wintertime (Hodnebrog et al., 2018; Lee et al., 2006; Rossabi & Helmig, 2018). These lifetimes are long enough that both MEK and its precursors can be transported into the remote marine atmosphere from terrestrial sources. To isolate clean air masses, we define a series of conservative estimates of CO background mixing ratios by region and season. In the Southern Ocean (SO), we define the background CO mixing ratio as 50 ppb in January and February and 60 ppb in July and August; in the South Atlantic (SA) and South Pacific (SP) we define the background CO mixing ratios as 55 ppb in January and February and 65 ppb in July and August; in the Western Tropical Pacific (WTP) the values are defined as 85 ppb during January and February and 70 ppb during July and August. These values were chosen considering the GLOBALVIEW-CO observations from the same year (GLOBALVIEW-CO, 2009) and do not reflect a specific CO percentile in the ATom data set; this choice was made because different regions and seasons sampled by ATom can have more or less data "above background," reflecting the number of polluted air masses sampled. We have examined the sensitivity of our results to the choice of background: Increasing background CO by 5 ppb makes little difference to our results, while reducing background values by 5 ppb reduces the number of clean observations and renders statistical analysis difficult in some regions and seasons, especially in the SA. This sensitivity is included in the text where relevant. We use these background values to eliminate recent influence from sources of MEK on land and thus isolate "clean" air masses in which CO is produced primarily from the oxidation of long-term reservoirs of natural and anthropogenic reservoir species. In the ATom 1 and 2 data sets in the regions of interest (including data above CO background), MEK is weakly correlated with CO ($r = 0.245$, $p = 2.5 \times 10^{-19}$) because the two species share several sources (biomass burning and alkane oxidation). In the context of these correlations, p is the probability that the null hypothesis of no relationship between the variables is correct. At CO mixing ratios at or below background, however, MEK and CO are not correlated in these regions ($r = 0.07$, $p = 0.07$).

We have grouped the ATom observations over the remote oceans by the regions shown in Figure 1. This figure also shows the clean-marine (colored) and anthropogenically influenced (gray) data points, as well as the vertical distribution of the sampling (color scale). Because we are attempting to identify clean air masses, we have restricted this study to four relatively remote and clean regions sampled by ATom: the WTP, the SP, the SA, and the SO. There are additional ATom data in the Eastern Tropical Pacific and Tropical Atlantic, but they are largely land influenced, and we omit them from this analysis. Stratospheric influences in the data set were minimal and were excluded by using only points below 10 km. We also tested our results by including only measurements where ozone <90 ppb to remove stratospheric influence; the results were unchanged.

2.2. Flux Calculations

We use a simplified two-layer model developed by Liss and Slater (1974) to calculate the air-sea exchange of MEK. This model, used in many air-sea flux schemes (Fischer et al., 2012; Johnson, 2010; Wang et al., 2019), parameterizes the flux of a gas into or out of the ocean based on windspeeds and concentration gradients. We supplement the original two-layer model with updated air (Johnson, 2010) and water (Nightingale et al., 2000) transfer velocities. The necessary variables for this parameterization were from in situ ATom observations taken at less than 200 m above sea level (temperature, pressure, atmospheric MEK mixing ratios, and windspeed), non-ATom observations (oceanic MEK mixing ratios, discussed below), and satellite observations (sea surface temperature [SST] and salinity). SSTs for the ATom-1 and ATom-2 time periods are from the Moderate Resolution Imaging Spectroradiometer-Aqua L3 11 micron SST product (Ocean Biology Processing Group, 2015; Werdell et al., 2013); salinity is from the Aquarius rain-corrected monthly sea surface salinity product for the relevant months in 2014 (the last year available from Aquarius) (JPL, 2015). We also re-ran the model using a regional mean surface windspeed from the Modern-Era Retrospective analysis for Research and Applications version 2 reanalysis (Gelaro et al., 2017) over the same time period, with similar results. All calculation inputs are included in the supporting information (Table S1).

3. Results

3.1. Multibasin Evidence for an Oceanic MEK Source

Figure 2 presents vertical profiles of MEK over the remote ocean regions sampled by the ATom missions. The data are presented in 1-km altitude bins and further classified by meteorological season. We define
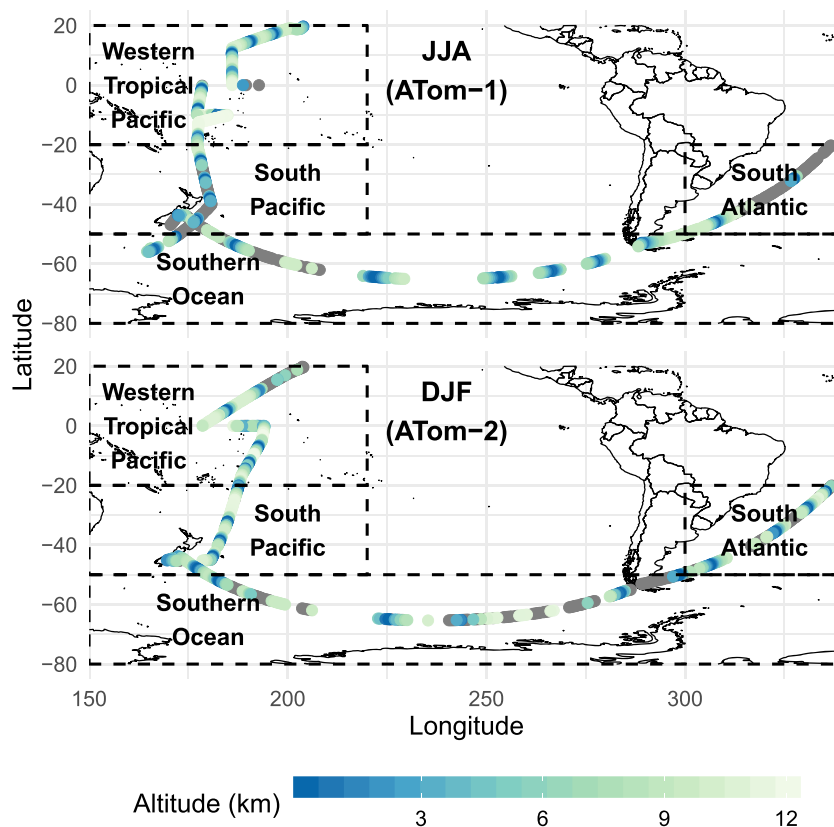
Figure 1. ATom-1 (July and august) and ATom-2 (January and February) sampling locations. Gray data points are classified as anthropogenically influenced and not included in our analysis. The colored points are at or below CO background as defined in the text and are classified as clean air masses (see text). The color scale shows the aircraft altitude. Data have been grouped into four coherent regions: Western tropical Pacific, South Pacific, Southern Ocean, and South Atlantic. Data not included in this figure had no values recorded due to instrument downtime for either the MEK mixing ratios or CO mixing ratios and has not been included in any of our analysis.

meteorological winter as December–February in the Northern Hemisphere and June–August in the Southern Hemisphere, while meteorological summer is the reverse. In the equatorial regions, this classification becomes less meaningful, but little seasonality was observed in the vertical profiles in those regions. We denote the 25th, 50th, and 75th percentile for each 1-km altitude bin and season. Solid colors denote the profile with a CO filter applied; in dashed lines we show the same statistics calculated using all of the data. In taking this approach, we assume that there is some atmospheric background profile, through which more polluted coherent air masses advect. By filtering out the polluted air signal and averaging across the region, we hope to visualize a profile that reflects only the regional emissions.

The vertical distribution of MEK over the remote oceans is consistent with a source at the surface and a sink aloft. The consistent profile shape is present during both summer and winter in all regions including the SO. Except in the tropics, the summer surface enhancement is generally larger than the winter surface enhancement. The SP and SO summer surface enhancements are larger than their winter counterparts. The highest median MEK surface mixing ratios were encountered in the SP, while the highest extremes in the unfiltered data were measured in the WTP; in the filtered data, both maxima were in the SP. The similarity in shapes between the CO-filtered and full-data vertical profiles in the middle and lower troposphere strengthens the evidence for an oceanic source; it also means that our analysis is not sensitive to the choice of background CO mixing ratio(s). The only major feature removed by filtering for CO occurs in the mid to lower troposphere during the SA winter is the MEK spike at 2 km in the full-data profile. Examination of other fire tracer mixing ratios observed with TOGA (HCN, CH_3CN) suggests that the source of this MEK enhancement was biomass burning. Additional examination of the n-butane and i-pentane abundances measured by TOGA shows that mixing ratios of these species are either negligible or very low and have the opposite
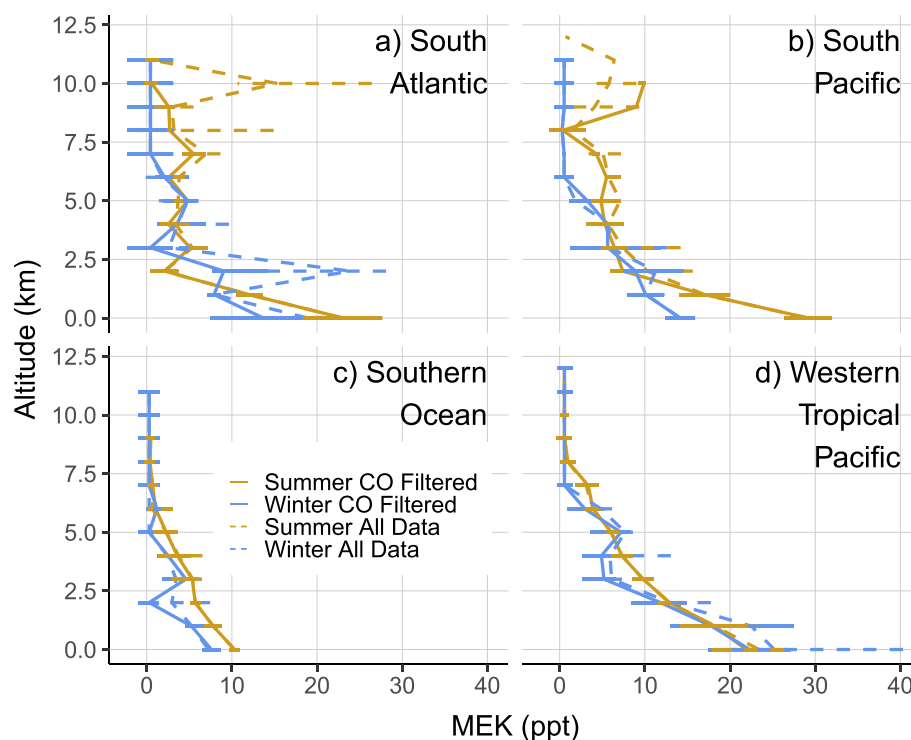
Figure 2. MEK observations from ATom-1 and ATom-2 in the a) South Atlantic, b) South Pacific, c) Southern Ocean, and d) Western tropical Pacific in 1-km altitude bins. Vertical lines connect the median value for each binned vertical km, and horizontal bars show the spread of the 25th and 75th percentiles. Blue lines summarize data from the meteorological winter (January and February in the northern hemisphere, July and august in the southern hemisphere) and orange lines summarize data from meteorological summer. The solid lines show the data from the CO-filtered air masses, where CO mixing ratios are at or below the regional background (as described text). Dashed lines present the same analysis using all available MEK data.

seasonality of that observed in MEK (i.e., concentrations are larger in the winter than the summer). The observed alkanes cannot explain the observed MEK signal unless we assume that all or almost all of the alkanes previously present in the air mass have already been oxidized away (Figure S1), and both our CO filter and the short residence times of the air mass within the marine boundary rule out this possibility. Further discussion of these observations is included in the Supplemental Material (Text S3). Sample sizes for each vertical level, region, and season are included in the supplemental material (Figure S2).

3.2. Possible Sources of Oceanic MEK

We suggest that there are at least two potential oceanic sources of MEK: (1) phytoplankton in the remote oceans and (2) another chemical or photochemical process in the surface ocean. If MEK were produced mostly by phytoplankton, we would expect to observe a correlation between the abundance of MEK and tracers for oceanic production. We calculated correlations between MEK and four OVOCs with documented ocean sources: methyl nitrate, acetone, acetaldehyde, and DMS. The atmospheric lifetimes of these species to chemical loss (primarily oxidation by OH and photodissociation) vary. The global mean lifetimes of methyl nitrate, acetone, and acetaldehyde, respectively, are 26 days (Fisher et al., 2018), 19 days (Brewer et al., 2017), and 20 hr (Millet et al., 2010); the mean atmospheric lifetime of DMS is 1–2 days (Kloster et al., 2006; Marandino, 2005). These lifetimes bracket the lifetime of MEK of 5–6 days to chemical loss at an OH concentration $\sim 1.5 \times 10^6$ cm^{-3} (Jordan et al., 2009; Yañez-Serrano et al., 2016). Figure 3 presents the correlation between the MEK and these species in CO-filtered air below 1 km in each of the regions in Figure 1. Because the TOGA and WAS sampling periods are different, each sample here represents a single profile-averaged value from both TOGA (for acetone, MEK, and acetaldehyde), WAS (for DMS and methyl nitrate), and Quantum Cascade Laser Spectrometer (for CO) under 1 km. Once filtered by the background CO mixing ratio, sample sizes are limited to 20 and 37 in the WTP and SO and to 25 and 14 in the SA and SP, respectively. To ensure the maximum reliability in the statistics, this analysis does not discriminate
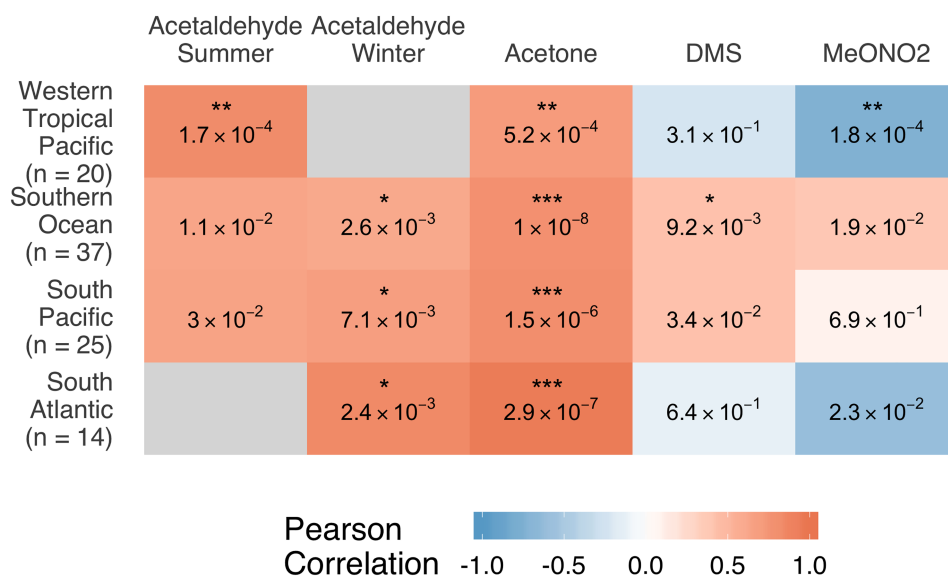
	Acetaldehyde Summer	Acetaldehyde Winter	Acetone	DMS	MeONO2
Western Tropical Pacific (n = 20)	** 1.7×10^{-4}		** 5.2×10^{-4}	3.1×10^{-1}	** 1.8×10^{-4}
Southern Ocean (n = 37)	1.1×10^{-2}	* 2.6×10^{-3}	*** 1×10^{-8}	* 9.2×10^{-3}	1.9×10^{-2}
South Pacific (n = 25)	3×10^{-2}	* 7.1×10^{-3}	*** 1.5×10^{-6}	3.4×10^{-2}	6.9×10^{-1}
South Atlantic (n = 14)		* 2.4×10^{-3}	*** 2.9×10^{-7}	6.4×10^{-1}	2.3×10^{-2}

Pearson Correlation -1.0   -0.5   0.0   0.5   1.0

Figure 3. Summary of Pearson correlation coefficients calculated based on the relationships between individual near-surface (<1 km) profile-averaged ATom observations of MEK and various species in CO-filtered air by region. Tiles are colored by the sign of the Pearson correlation coefficient in that region. Gray tiles indicate that the sample size is too small for correlation to be meaningful ($n < 10$). Total sample n is shown on the y axis for each region. The p value is shown on each tile, along with stars showing the relative p-value magnitudes in each region: One star corresponds to a p value between 1×10^{-3} and 1×10^{-2}, two stars 1×10^{-3} and 1×10^{-4}, and three stars $p \leq 1 \times 10^{-4}$. Acetaldehyde has been separated into winter and summer correlations because the distributions differ between seasons in all regions, which is not true for the other three species shown; as such, the n values given for each region refer to the total sample size of winter and summer combined.

between seasons—all CO-filtered data are combined in this analysis regardless of season. The one exception is the acetaldehyde-MEK correlation, which shows dramatic differences between seasons. Scatterplots showing the complete data set summarized in Figure 3 are included in the supporting information (Figures S3–S6).

Figure 3 shows that MEK and acetone are well correlated across ocean basins, while the other species show more heterogeneity in the relationships to MEK in this data set. Correlation coefficients between acetone and MEK range from 0.72 to 0.95, three of which have p values $\leq 1.5 \times 10^{-6}$. This robust correlation in CO-filtered air across ocean regions suggests that acetone and MEK share an oceanic source. This source is sufficiently large that observed mixing ratios of MEK are around 10% of that of acetone in the remote marine boundary layer. Given the disparity in lifetime between these two compounds, the flux of MEK out of the surface layer must be greater than 10% of that of acetone. Acetaldehyde and MEK are also positively correlated but less strongly than acetone and MEK. Unlike the MEK-acetone case, the correlations between MEK and acetaldehyde differ seasonally. For this reason, we present the seasonal correlations for acetaldehyde in each region and season in which sample sizes were sufficiently large. A possible explanation for this correlation is that the photooxidation of MEK can produce acetaldehyde (Calvert et al., 2011), and so we might expect the two species to appear correlated even without a common source. To examine this possibility, we used a back trajectory analysis (Bowman, 1993; Bowman et al., 2013; Bowman & Carrie, 2002) to estimate the mean time that a sampled air mass had been in contact with the oceanic boundary layer. The specifics of this procedure (Text S2), and the results of the modeling (Figures S7 and S8), are included in the supporting information. In all locations and seasons studied, the median air mass sampled had been in the boundary layer for less than 5 days. Given the relatively long atmospheric lifetime of MEK, the correlations observed are still likely to represent a common source rather than the atmospheric production of acetaldehyde from MEK. In the WTP and SP during summer, a small number of air masses sampled were within the boundary layer for between 12 and 15 days. Therefore, it is possible that the particularly strong correlation shown between MEK and acetaldehyde in the WTP summer might be the result MEK photooxidation; in light of the similar correlations shown in other regions, we still believe that the weight of evidence rests on the side of a common oceanic source for the two species. Methyl nitrate shows a strong negative correlation with

MEK in the WTP. This may simply be an artifact of the greater variability of methyl nitrate in these regions (mixing ratios range from 4 to 88 ppt for methyl nitrate and 5 to 39 ppt for MEK), but the robustness of the negative correlation observed does suggest the possibility of some real and unexplained inverse relationship between MEK and methyl nitrate emissions. In our analysis, DMS is mostly uncorrelated with MEK, with the sole exception being a weak positive correlation observed in the SP ($r = 0.47$, $p = 0.02$). This correlation may simply reflect the summertime increases in both MEK and DMS in the region (see Figure S4 in the supporting information) and the near-zero DMS values observed during winter. Because the rate coefficient for the reaction with OH is ~10× lower for MEK than DMS (Burkholder et al., 2015) and our back-trajectory modeling shows that most air masses sampled had been in contact with the oceanic boundary layer for more than a day (the mean lifetime of DMS; see Figure S7 in the supporting information), we cannot rule out the possibility that MEK and DMS were coemitted in these regions and over time the coemitted DMS reacted away and was not observed by our study. However, given that acetaldehyde did show a correlation with MEK despite having a similar atmospheric lifetime to DMS, we believe that the emissions of DMS and MEK are unlikely to be correlated. Given the observed connections between the decline of phytoplankton blooms and acetone emissions (Sinha et al., 2007), it is possible that a time-lagged correlation between MEK and DMS might exist; however, the temporal resolution of our data does not allow the analysis necessary to observe such a connection. These results are insensitive to the choice of background CO. Based on this analysis, our observed correlations between MEK and acetone, as well as those between MEK and acetaldehyde, are robust and consistent with the three species sharing similar oceanic sources.

We are only aware of two papers detailing observations of MEK in seawater. Swan et al. (2016) sampled Australian coral reefs and observed concentrations of MEK in seawater ranging from 102 to 119 nM. Swan et al. (2016) also documented similar seawater acetone concentrations (74–183 nM), which are an order of magnitude higher than the range of previously estimated open-ocean mixed-layer acetone concentrations (Brewer et al., 2017; Fischer et al., 2012) and roughly two to four times as high as the highest previous measurements in the open ocean (Tanimoto et al., 2014). Since acetone concentrations are observed to be lower in the pelagic environment than in coral reef seawater, we assume that open-ocean MEK concentrations are also much lower than those observed by Swan et al. (2016). Therefore, we treat their observation as an upper limit for our model calculations. Schlundt et al. (2017) report median MEK concentrations of ~0.88 nM in the Sulu and South China seas. These concentrations are smaller than the lower end of acetone values in the open ocean by a factor of ~3 (Brewer et al., 2017).

The air-sea exchange of MEK can also be represented using a flux model (section 2.2). When we estimate the flux of MEK using realistic ocean conditions with seawater MEK concentrations similar to those observed by Schlundt et al. (2017), the model produces a small net positive flux of MEK in all seasons and regions examined. For all regions and both seasons, the ocean does not take up MEK until the seawater concentration of MEK falls below ~0.3 nM. These model results are presented in greater detail in the Supplemental Material (Figure S8).

While seawater MEK concentrations are as of now mostly unknown, existing measurements suggest that MEK shares a similar oceanic abundance to acetone. The lowest acetone observed in the surface ocean ranges from 2 to 5 nM, as summarized by Brewer et al. (2017). Our calculations suggest that ocean regions shown in Figure 1 likely serve as a net source of MEK to the atmosphere. For comparison purposes, a 3-nM average seawater MEK concentration in the SO implies a ~0.5-Tg annual source from that region. Using 0.88 nM (Schlundt et al., 2017) instead gives a ~0.06-Tg annual source over the SO.

4. Conclusions

Using data from CO-filtered air masses sampled in the ATom-1 and ATom-2 field campaigns, we provide evidence that the ocean is a source of MEK to the atmosphere. Outside the tropics, this source is more pronounced during summer than winter; less seasonality is observed in the tropics. MEK in the regions we examined is sometimes weakly correlated with DMS—a reliable tracer of marine biological activity. Ocean-produced MEK is strongly correlated with acetone and slightly less strongly correlated with acetaldehyde, which suggests the three species could share similar sources. Acetone and MEK have similar abundances in the only existing measurements of both species in seawater, providing additional evidence of a

similar source, and even a small concentration of MEK in surface seawaters results in a flux of MEK out of the surface waters.

ATom observations suggest that MEK′ flux out of the ocean is >10% of that of acetone. As MEK oxidation is a source of acetaldehyde in the troposphere, this oceanic MEK might serve as a source of acetaldehyde in regions where current sources fail to explain observations (Wang et al., 2019; Wolfe et al., 2019). Quantification of the sources and sinks of MEK in the oceans is needed to improve our understanding of MEK and its implications for global oxidation capacity.

5. Data Availability Statement

ATom observational data used in this study including flight tracks, trace gas observations, and Lagrangian model output are publicly accessible via ESPO data archive at https://espo.nasa.gov/atom/archive/browse/atom/id3/DC8.

References

Apel, E. C. (2003). A fast-GC/MS system to measure C2to C4 carbonyls and methanol aboard aircraft. *Journal of Geophysical Research*, *108*(D20), 8794. https://doi.org/10.1029/2002JD003199

Apel, E. C., Hornbrook, R. S., Hills, A. J., Blake, N. J., Barth, M. C., Weinheimer, A., et al. (2015). Upper tropospheric ozone production from lightning NO$_x$-impacted convection: Smoke ingestion case study from the DC3 campaign. *Journal of Geophysical Research: Atmospheres*, *120*(6), 2505–2523. https://doi.org/10.1002/2014JD022121

Barletta, B., Nissenson, P., Meinardi, S., Dabdub, D., Sherwood Rowland, F., VanCuren, R. A., et al. (2011). HFC-152a and HFC-134a emission estimates and characterization of CFCs, CFC replacements, and other halogenated solvents measured during the 2008 ARCTAS campaign (CARB phase) over the south coast Air Basin of California. *Atmospheric Chemistry and Physics*, *11*(6), 2655–2669. https://doi.org/10.5194/acp-11-2655-2011

Bowman, K. P. (1993). Large-scale isentropic mixing properties of the Antarctic polar vortex from analyzed winds. *Journal of Geophysical Research*, *98*(D12), 23,013–23,027. https://doi.org/10.1029/93JD02599

Bowman, K. P., & Carrie, G. D. (2002). The mean-meridional transport circulation of the troposphere in an idealized GCM. *Journal of the Atmospheric Sciences*, *59*(9), 1502–1514. https://doi.org/10.1175/1520-0469(2002)059<1502:TMMTCO>2.0.CO;2

Bowman, K. P., Lin, J. C., Stohl, A., Draxler, R., Konopka, P., Andrews, A., & Brunner, D. (2013). Input data requirements for Lagrangian trajectory models. *Bulletin of the American Meteorological Society*, *94*, 1051–1058.

Brewer, J. F., Bishop, M., Kelp, M., Keller, C., Ravishankara, A. R., & Fischer, E. V. (2017). A sensitivity analysis of key factors in the modeled global acetone budget. *Journal of Geophysical Research: Atmospheres*, *122*, 2043–2058. https://doi.org/10.1002/2016JD025935

Brewer, J. F., Papanastasiou, D. K., Burkholder, J. B., Fischer, E. V., Ren, Y., Mellouki, A., & Ravishankara, A. R. (2019). Atmospheric photolysis of methyl ethyl, diethyl, and propyl ethyl ketones: Temperature dependent UV absorption cross sections. *Journal of Geophysical Research: Atmospheres*, *124*, 2019JD030391. https://doi.org/10.1029/2019JD030391

Burkholder, J. B., Sander, S. P., Abbatt, J., Barker, J. R., Huie, R. E., Kolb, C. E., et al. (2015). Chemical kinetics and photochemical data for use in atmospheric studies. In *JPL Publication 15–10* (Chap. 1, Vol. 18, pp. 1–326). Pasadena: Jet Propulsion Laboratory.

Calvert, J. G., Mellouki, A., Orlando, J. J., Pilling, M. J., & Wallington, T. J. (2011). *The Mechanisms of Atmospheric Oxidation of the Oxygenates*. New York: Oxford University Press.

Cappellin, L., Algarra Alarcon, A., Herdlinger-Blatt, I., Biasioli, F., Martin, S., Loreto, F., & McKinney, K. (2016). Field observations of volatile organic compound (VOC) exchange in red oaks. *Atmospheric Chemistry and Physics Discussions*, 1–55. https://doi.org/10.5194/acp-2016-901

Challenger, F. (1952). Biological methylation. In F. F. Nord (Ed.), *Advances in Enzymology and Related Areas of Molecular Biology* (pp. 429–491). Hoboken, NJ, USA: John Wiley & Sons, Inc. https://doi.org/10.1002/9780470122570.ch8

Chen, X., Millet, D. B., Singh, H. B., Wisthaler, A., Apel, E. C., Atlas, E. L., et al. (2019). On the sources and sinks of atmospheric VOCs: An integrated analysis of recent aircraft campaigns over North America. *Atmospheric Chemistry and Physics*, *19*(14), 9097–9123. https://doi.org/10.5194/acp-19-9097-2019

Colman, J. J., Swanson, A. L., Meinardi, S., Sive, B. C., Blake, D. R., & Rowland, F. S. (2001). Description of the analysis of a wide range of volatile organic compounds in whole air samples collected during PEM-tropics a and B. *Analytical Chemistry*, *73*(15), 3723–3731. https://doi.org/10.1021/ac010027g

Dixon, J. L., Beale, R., & Nightingale, P. D. (2013). Production of methanol, acetaldehyde, and acetone in the Atlantic Ocean. *Geophysical Research Letters*, *40*(17), 4700–4705. https://doi.org/10.1002/grl.50922

Dixon, J. L., Beale, R., Sargeant, S. L., Tarran, G. A., & Nightingale, P. D. (2014). Microbial acetone oxidation in coastal seawater. *Frontiers in Microbiology*, *5*, 243. https://doi.org/10.3389/fmicb.2014.00243

Fischer, E. V., Jacob, D. J., Millet, D. B., Yantosca, R. M., & Mao, J. (2012). The role of the ocean in the global atmospheric budget of acetone. *Geophysical Research Letters*, *39*, L01807. https://doi.org/10.1029/2011GL050086

Fisher, J. A., Atlas, E. L., Barletta, B., Meinardi, S., Blake, D. R., Thompson, C. R., et al. (2018). Methyl, ethyl, and propyl nitrates: Global distribution and impacts on reactive nitrogen in remote marine environments. *Journal of Geophysical Research: Atmospheres*, *123*(21), 12,429–12,451. https://doi.org/10.1029/2018JD029046

Gelaro, R., McCarty, W., Suárez, M. J., Todling, R., Molod, A., Takacs, L., et al. (2017). The modern-era retrospective analysis for research and applications, version 2 (MERRA-2). *Journal of Climate*, *30*(14), 5419–5454. https://doi.org/10.1175/JCLI-D-16-0758.1

GLOBALVIEW-CO. (2009). *GLOBALVIEW-CO: Cooperative Atmospheric Data Integration Project - Carbon Monoxide*. Boulder, Colorado: NOAA ESRL. Retrieved from aftp.cmdl.noaa.gov, Path: products/globalview/co

Hodnebrog, Ø., Dalsøren, S. B., & Myhre, G. (2018). Lifetimes, direct and indirect radiative forcing, and global warming potentials of ethane (C_2H_6), propane (C_3H_8), and butane (C_4H_{10}). *Atmospheric Science Letters*, *19*(2), e804. https://doi.org/10.1002/asl.804

Johnson, M. T. (2010). A numerical scheme to calculate temperature and salinity dependent air-water transfer velocities for any gas. *Ocean Science*, *6*(4), 913–932. https://doi.org/10.5194/os-6-913-2010

Jordan, C., Fitz, E., Hagan, T., Sive, B., Frinak, E., Haase, K., et al. (2009). Long-term study of VOCs measured with PTR-MS at a rural site in New Hampshire with urban influences. *Atmospheric Chemistry and Physics*, *9*, 4677–4697.

JPL. (2015). Aquarius CAP level 3 sea surface salinity rain corrected standard mapped image monthly data V4.0. NASA physical oceanography DAAC. https://doi.org/10.5067/AQR40-3QMCS

Kieber, R. J., Zhou, X., & Mopper, K. (1990). Formation of carbonyl compounds from UV-induced photodegradation of humic substances in natural waters: Fate of riverine carbon in the sea. *Limnology and Oceanography*, *35*(7), 1503–1515.

Kloster, S., Feichter, J., Maier-Reimer, E., Six, K. D., Stier, P., & Wetzel, P. (2006). DMS cycle in the marine ocean-atmosphere system—A global model study. *Biogeosciences*, *3*, 29–51.

Lee, B. H., Munger, J. W., Wofsy, S. C., & Goldstein, A. H. (2006). Anthropogenic emissions of nonmethane hydrocarbons in the northeastern United States: Measured seasonal variations from 1992–1996 and 1999–2001. *Journal of Geophysical Research*, *111*, D20307. https://doi.org/10.1029/2005JD006172

Liss, P., & Slater, P. G. (1974). Flux of gases across the air-sea Interface. *Nature*, *247*, 181–184.

Lovelock, J. E., Maggs, R. J., & Rasmussen, R. A. (1972). Atmospheric dimethyl sulphide and the natural Sulphur cycle. *Nature*, *237*(5356), 452–453. https://doi.org/10.1038/237452a0

Marandino, C. A. (2005). Oceanic uptake and the global atmospheric acetone budget. *Geophysical Research Letters*, *32*, L15806. https://doi.org/10.1029/2005GL023285

Martinez, R. D., Buitrago, A. A., Howell, N. W., Hearn, C. H., & Joens, J. A. (1992). The near U.V. absorption spectra of several aliphatic aldehydes and ketones at 300 K. *Atmospheric Environment*, *26A*(5), 785–792.

McKeen, S. A., Gierczak, T., Burkholder, J. B., Wennberg, P. O., Hanisco, T. F., Keim, E. R., et al. (1997). The photochemistry of acetone in the upper troposphere: A source of odd-hydrogen radicals. *Geophysical Research Letters*, *24*(24), 3177–3180. https://doi.org/10.1029/97GL03349

Millet, D. B., Guenther, A., Siegel, D. A., Nelson, N. B., Singh, H. B., de Gouw, J. A., et al. (2010). Global atmospheric budget of acetaldehyde: 3-D model analysis and constraints from in-situ and satellite observations. *Atmospheric Chemistry and Physics*, *10*(7), 3405–3425. https://doi.org/10.5194/acp-10-3405-2010

Moore, R. M., & Blough, N. V. (2002). A marine source of methyl nitrate. *Geophysical Research Letters*, *29*(15), 1737. https://doi.org/10.1029/2002GL014989

Nemecek-Marshall, M., Wojciechowski, C., Kuzma, J., Silver, G. M., & Fall, R. (1995). Marine vibrio species produce the volatile organic compound acetone. *Applied and Environmental Microbiology*, *61*(1), 44–47.

Neumaier, M., Ruhnke, R., Kirner, O., Ziereis, H., Stratmann, G., Brenninkmeijer, C. A. M., & Zahn, A. (2014). Impact of acetone (photo) oxidation on HOx production in the UT/LMS based on CARIBIC passenger aircraft observations and EMAC simulations. *Geophysical Research Letters*, *41*(9), 3289–3297. https://doi.org/10.1002/2014GL059480

Nevitt, G. A., Veit, R. R., & Kareiva, P. (1995). Dimethyl sulphide as a foraging cue for Antarctic Procellariiform seabirds. *Nature*, *376*(6542), 680–682. https://doi.org/10.1038/376680ao

Nightingale, P. D., Malin, G., Law, C. S., Watson, A. J., Liss, P. S., Liddicoat, M. I., et al. (2000). In situ evaluation of air-sea gas exchange parameterizations using novel conservative and volatile tracers. *Global Biogeochemical Cycles*, *14*(1), 373–387. https://doi.org/10.1029/1999GB900091

Ocean Biology Processing Group. (2015). MODIS aqua level 3 SST thermal IR annual 4km daytime v2014.0. NASA physical oceanography DAAC. https://doi.org/10.5067/MODSA-AN4D4

Romero, M. T. B., Blitz, M. A., Heard, D. E., Pilling, M. J., Price, B., Seakins, P. W., & Wang, L. (2005). Photolysis of methylethyl, diethyl and methylvinyl ketones and their role in the atmospheric HOx budget. *Faraday Discussions*, *130*, 73. https://doi.org/10.1039/b419160a

Rossabi, S., & Helmig, D. (2018). Changes in atmospheric butanes and pentanes and their isomeric ratios in the continental United States. *Journal of Geophysical Research: Atmospheres*, *123*(7), 3772–3790. https://doi.org/10.1002/2017JD027709

Santoni, G. W., Daube, B. C., Kort, E. A., Jiménez, R., Park, S., Pittman, J. V., et al. (2014). Evaluation of the airborne quantum Cascade laser spectrometer (QCLS) measurements of the carbon and greenhouse gas suite—CO_2, CH_4, N_2O, and CO—During the CalNex and HIPPO campaigns. *Atmospheric Measurement Techniques Discussions*, *6*(6), 9689–9734. https://doi.org/10.5194/amtd-6-9689-2013

Schlundt, C., Tegtmeier, S., Lennartz, S. T., Bracher, A., Cheah, W., Krüger, K., et al. (2017). Oxygenated volatile organic carbon in the western Pacific convective center: Ocean cycling, air–sea gas exchange and atmospheric transport. *Atmospheric Chemistry and Physics*, *17*(17), 10,837–10,854. https://doi.org/10.5194/acp-17-10837-2017

Singh, H. B., Kanakidou, M., Crutzen, P. J., & Jacob, D. J. (1995). High concentrations and photochemical fate of oxygenated hydrocarbons in the global troposphere. *Nature*, *378*, 50–54.

Singh, H. B., Salas, L. J., Chatfield, R. B., Czech, E., Fried, A., Walega, J., et al. (2004). Analysis of the atmospheric distribution, sources, and sinks of oxygenated volatile organic chemicals based on measurements over the Pacific during TRACE-P. *Journal of Geophysical Research*, *109*(D15), D15S07. https://doi.org/10.1029/2003jd003883

Sinha, V., Williams, J., Meyerhofer, M., Riebesell, U., Paulino, A. I., & Larsen, A. (2007). Air-Sea fluxes of methanol, acetone, acetaldehyde, isoprene, and DMS from a Norwegian fjord following a phytoplankton bloom in a mesocosm experiment. *Atmospheric Chemistry and Physics*, *7*, 739–755.

Swan, H. B., Crough, R. W., Vaattovaara, P., Jones, G. B., Deschaseaux, E. S. M., Eyre, B. D., et al. (2016). Dimethyl sulfide and other biogenic volatile organic compound emissions from branching coral and reef seawater: Potential sources of secondary aerosol over the great barrier reef. *Journal of Atmospheric Chemistry*, *73*(3), 303–328. https://doi.org/10.1007/s10874-016-9327-7

Tanimoto, H., Kameyama, S., Omori, Y., Inomata, S., & Tsunogai, U. (2014). High-resolution measurement of volatile organic compounds dissolved in seawater using equilibrator inlet-proton transfer reaction-mass spectrometry (EI-PTR-MS), 89–115. https://doi.org/10.5047/w-pass.a02.001

Wang, S., Hornbrook, R. S., Hills, A., Emmons, L. K., Tilmes, S., Lamarque, J.-F., et al. (2019). Atmospheric acetaldehyde: Importance of air-sea exchange and a missing source in the remote troposphere. *Geophysical Research Letters*, *46*(10), 5601–5613. https://doi.org/10.1029/2019GL082034

Wennberg, P. O., Hanisco, T. F., Jaegle, L., Jacob, D. J., Hintsa, E. J., Lanzendorf, E. J., et al. (1998). Hydrogen radicals, nitrogen radicals, and the production of O_3 in the upper troposphere. *Science*, *279*(5347), 49–53. https://doi.org/10.1126/science.279.5347.49

Werdell, P. J., Franz, B. A., Bailey, S. W., Feldman, G. C., Boss, E., Brando, V. E., et al. (2013). Generalized Ocean color inversion model for retrieving marine inherent optical properties. *Applied Optics*, *52*(10), 2019–2037. https://doi.org/10.1364/AO.52.002019

Wolfe, G. M., Nicely, J. M., Clair, J. M. S., Hanisco, T. F., Liao, J., Oman, L. D., et al. (2019). Mapping hydroxyl variability throughout the global remote troposphere via synthesis of airborne and satellite formaldehyde observations. *Proceedings of the National Academy of Sciences*, *116*(23), 11,171–11,180. https://doi.org/10.1073/pnas.1821661116

Yañez-Serrano, A. M., Nolscher, A. C., Bourtsoukidis, E., Derstroff, B., Zanoni, N., Gros, V., et al. (2016). Atmospheric mixing ratios of methyl ethyl ketone (2-butanone) in tropical, boreal, temperate, and marine environments. *Atmospheric Chemistry and Physics*, *16*(17), 10,965–10,984. https://doi.org/10.5194/acp-16-10965-2016

Yang, M., Beale, R., Liss, P., Johnson, M., Blomquist, B., & Nightingale, P. (2014). Air–sea fluxes of oxygenated volatile organic compounds across the Atlantic Ocean. *Atmospheric Chemistry and Physics*, *14*(14), 7499–7517. https://doi.org/10.5194/acp-14-7499-2014

Yang, M., Bell, T. G., Blomquist, B. W., Fairall, C. W., Brooks, I. M., & Nightingale, P. D. (2016). Air-sea transfer of gas phase controlled compounds. *IOP Conference Series: Earth and Environmental Science*, *35*, 012011. https://doi.org/10.1088/1755-1315/35/1/012011

Zhou, X., & Mopper, K. (1997). Photochemical production of low-molecular-weight-carbonyl compounds in seawater and surface micro-layer and their air-sea exchange. *Marine Chemistry*, *56*, 201–213.